Noise and Fuel Burn Reduction Potential of an Innovative Subsonic Transport Configuration

Yueping Guo*
Boeing Research & Technology, Huntington Beach, CA 92647

Craig L. Nickol†, and Russell H. Thomas‡
NASA Langley Research Center, Hampton, VA 23681

A study is presented for the noise and fuel burn reduction potential of an innovative double deck concept aircraft with two three-shaft direct-drive turbofan engines. The engines are mounted from the fuselage so that the engine inlet is over the main wing. It is shown that such an aircraft can achieve a cumulative Effective Perceived Noise Level (EPNL) about 28 dB below the current aircraft noise regulations of Stage 4. The combination of high bypass ratio engines and advanced wing design with laminar flow control technologies provide fuel burn reduction and low noise levels simultaneously. For example, the fuselage mounted engine position provides more than 4 EPNLdB of noise reduction by shielding the inlet radiated noise. To identify the potential effect of noise reduction technologies on this concept, parametric studies are presented to reveal the system level benefits of various emerging noise reduction concepts, for both engine and airframe noise reduction. These concepts are discussed both individually to show their respective incremental noise reduction potential and collectively to assess their aggregate effects on the total noise. Through these concepts approximately about 8 dB of additional noise reduction is possible, bringing the cumulative noise level of this aircraft to 36 EPNLdB below Stage 4, if the entire suite of noise reduction technologies would mature to practical application. In a final step, an estimate is made for this same aircraft concept but with higher bypass ratio, geared, turbofan engines. With this geared turbofan propulsion system, the noise is estimated to reach as low as 40-42 dB below Stage 4 with a fuel burn reduction of 43-47% below the 2005 best-in-class aircraft baseline. While just short of the NASA N+2 goals of 42 dB and 50% fuel burn reduction, for a 2025 in service timeframe, this assessment shows that this innovative concept warrants refined study. Furthermore, this design appears to be a viable potential future passenger aircraft, not only in meeting the regulatory requirements, but also in competing with aircraft of different advanced designs within this N+2 timeframe and goal framework.

Nomenclature

AOA	=	angle of attack
B27	=	over-the-wing, mid-fuselage engine mount aircraft configuration, Boeing concept
BPR	=	engine bypass ratio, mass flow of fan to mass flow of core
BWB	=	Blended-Wing-Body, Boeing specific design
D	=	fan nozzle diameter
dB	=	decibel
ERA	=	NASA's Environmentally Responsible Aviation Project
EPNL	=	effective perceived noise level, decibels
FPR	=	fan pressure ratio
GTF	=	Geared Turbofan, Pratt & Whitney ultra high bypass engine
HWB	=	Hybrid Wing Body, generic term
LSAF	=	Low Speed Aeroacoustic Facility, Boeing

* Technical Fellow, Acoustics Technology, 5301 Bolsa Ave, Huntington Beach, CA, AIAA Associate Fellow
† Senior Research Engineer, Aeronautical Systems Analysis Branch, MS 442, AIAA Senior Member
‡ Senior Research Engineer, Aeroacoustics Branch, MS 461, AIAA Senior Member

M = mean flow Mach number
OTR/SV = Over-the-rotor and soft vane liner treatment for fan noise reduction, NASA
PNLT = tone corrected perceived noise level, decibels
SPL = sound pressure level
TE = trailing edge
UHB = ultra high bypass ratio

I. Introduction

Turbofan engine technology development for aircraft propulsion continues advancing towards higher bypass ratios, driven by fuel efficiency, but also with the acoustic benefit of lower jet noise levels from the reduced jet exhaust velocity. High bypass ratio engines, however, have their own challenges. At the aircraft system level, one example is the large diameter of the engines that makes the under-the-wing mounting of conventional aircraft configurations difficult. For noise, potential adverse effects of the large fan diameter include the inherently low tonal frequencies that are more difficult to suppress, the potential increases in the tonal amplitudes, the reduced liner area due to the shortened inlet length necessary to reduce drag and maintain the engine weight, and the increase in the number of cut-on modes in the fan inlet. All these are currently active research topics and various options for resolving these issues are being proposed and studied. One option to potentially resolve the constraints on engine size due to the typical under-the-wing engine installation is the configuration with the engines mounted on the fuselage and above the wings, an innovative aircraft concept detailed in Ref 1, where various other benefits associated with this design are also predicted.

In this study, a detailed assessment will be given on the system noise and fuel burn potential of this advanced tube-and-wing aircraft design with turbofan engine propulsion. The design is differentiated from the conventional configuration by mounting the engines from the fuselage behind but above the wings so that the noise from the inlet is shielded by the wing. The fuselage has a double deck with passengers and cockpit on the upper deck and a passenger and a cargo bay on the lower deck. The engine pylon structure at the mid-fuselage position is integrated through the deck. Both the airframe and the engine design of this concept resulted from a comprehensive study (Ref 1) and followed practical design principles to ensure the feasibility for realistic application. The designs, however, also included advanced technologies that are not fully mature now but are in active development and are expected to mature and enter service in the next decade or so. For example, the engines are designed for a bypass ratio of 13, the wings are implemented with laminar flow control devices, and the high lift system uses Krueger slats, all of which are currently in active development and are expected to have significant inherent acoustic and fuel efficiency benefits. Thus, the design both satisfies practical feasibility and incorporates emerging technologies, which is an aspect of aircraft system noise assessment also emphasized in studies of Refs 1-3. The study of Ref 1 was conducted for NASA's Environmentally Responsible Aviation (ERA) Project and that concept was termed the 0027A. In this current study, a slightly more aggressive version is used and it will be simply referred to as the B27. This B27 concept is an unconventional concept, certainly compared to the typical engine-under-wing type, however it is still fundamentally a tube-and-wing type similar in that way to that of the conventional engine-under-wing aircraft configuration.

NASA's ERA Project (Ref 4) has focused since 2009 on developing and demonstrating technologies for integrated aircraft systems that could meet simultaneously aggressive goals for fuel burn, noise, and emissions. The fuel burn goal is for a reduction of fuel burn of 50% relative to a best-in-class aircraft in 2005, the noise goal is 42 dB cumulative relative to the Stage 4 requirement, and the emissions goal is for a reduction of 75% in NOx below the CAEP 6 (Committee on Aviation Environmental Protection) standard. The target date is 2020 for key technologies to be at a technology readiness level (TRL) of 4-6 (system or sub-system prototype demonstrated in a relevant environment). This corresponds to a projected aircraft entry into service of 2025. These goals and timeframe are defined by NASA with the term N+2. The noise goal has been seen as a significant challenge and it has been thought through past research that only a configuration change would enable the 42 dB noise goal to be achieved and that the Hybrid Wing Body aircraft configuration, together with advanced technologies, would be the most likely (Refs 5-7). A simultaneous question has been if or under what technical framework would a configuration that was basically a tube-and-wing type be able to demonstrate a technical roadmap to reaching the 42 dB noise goal.

It will be shown that this advanced B27 aircraft concept can achieve a cumulative EPNL level about 28 dB below the current noise regulations of Stage 4, a comfortable margin to the current aircraft noise regulations, and to the potentially more stringent regulations in the next decade or so, which makes the configuration viable in meeting current and anticipated noise regulations. The low noise levels also make this aircraft acoustically competitive to

conventional aircraft designs. For comparison, it can be noted that the latest generations of commercial aircraft in service, such as the Boeing 787 and the Airbus 380, have cumulative EPNL margins to Stage 4 on the order of 16 to 20 dB. This margin of course can be expected to increase for future aircraft that are in active development, aided both by better high lift system design and by more advanced turbofan engines. With the expected technological advances, the under-the-wing installation configuration may be able to achieve a margin to Stage 4 of perhaps as much as 23 to 28 dB (Ref 1) by the NASA N+2 timeframe. This would give the B27 studied here a competitive advantage in acoustics by virtue of having, at least, the lowest levels of noise compared to conventional configurations. It will be shown that this B27 aircraft can provide at least 4 EPNLdB of noise reduction just from the configuration change alone, with all else equal.

The cumulative EPNL of 28 dB below Stage 4 for the baseline configuration is achieved without considering various emerging noise reduction technologies that are currently in development and have the potential to further reduce noise. An additional noise assessment is performed to identify the potential impact of a suite of these technologies that are well matched with the B27. These technologies all have the potential to provide 8 dB of additional noise reduction and bring the cumulative EPNL of this aircraft to 36 dB below Stage 4. However, it is important to emphasize that this assumes that the entire suite of noise reduction technologies would all mature for practical application in the next decade or so, a very challenging and aggressive assumption.

In a final analysis step, the B27 concept is configured with geared turbofan engines of a higher bypass ratio, about 15. This engine technology is also considered within the NASA N+2 technology and timeframe and is consistent with similar studies including those of Ref 1. Including the impact of the same suite of noise reduction technologies, the B27 with geared turbofan engines is estimated to reach 40-42 dB below Stage 4. A fuel burn assessment of this final configuration is performed and it will be shown to have a fuel burn reduction of between 43-47% from the levels of aircraft currently in service.

II. Baseline Configuration

The baseline configuration of the advanced tube-and-wing design results from a comprehensive design study (Ref 1), following the best practice in aircraft design as well as incorporating potential technologies that are likely to mature in the next decade or so, namely, in the 2025 entry-into-service timeframe of NASA's N+2 goals. This allows the design to be practically feasible, to meet various mission requirements, and to achieve a good balance between the goals for the reductions of fuel burn, noise and emissions. The baseline configuration is the tube-and-wing design with two three-spool direct-drive turbofan engines mounted on the sides of the fuselage, behind and above the wings, as illustrated in Figure 1. The details of the design have been discussed in Ref 1. The basic characteristics are summarized in Table 1.

The design details that affect the acoustic characteristics of the aircraft are summarized in Table 2. The aircraft is a tube-and-wing design similar to most of the large commercial aircraft currently in service, but it has a high double-deck fuselage. The aircraft has high aspect ratio wings including winglets, implemented with laminar flow control devices, to provide sufficient lift for the aircraft to land at speeds up to 20 knots lower than the typical landing speed of current generation of aircraft of comparable size and functionality. The lower approach speed reduces the airframe noise at approach conditions. Its high lift system consists of continuous single slotted trailing edge flaps and full-span, three position Krueger slats that are sealed for takeoff and open for landing, lowering the levels of two major airframe noise components. The landing gears are four-wheel and two-wheel designs respectively for the main and nose gear. The specific engine mounting configuration has various acoustic benefits; the absence of wing reflection of engine noise from the exhaust and jet noise, the shielding of inlet fan noise by the wings, and the shielding of the engine noise by the fuselage at sideline positions. The engine design follows the trend towards higher bypass ratio and lower fan pressure ratio, which are respectively 13.5 and 1.6 for this engine design, as also listed in Table 1. This helps reduce the jet noise because of the low exhaust flow velocity. Advanced liner treatments are included in the engine design for noise suppression.

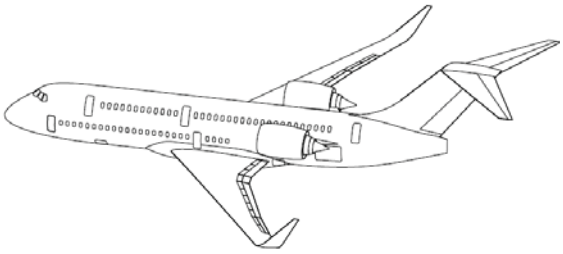

Figure 1. Illustration of the B27 advanced tube-and-wing aircraft design.

The baseline airframe and engine designs were mainly driven by the mission requirements of the aircraft and the design goals of fuel savings and emission reduction (Ref 1). Acoustics was considered in the designs only on the conceptual level with engineering experience. Thus, there was no acoustic optimization or parametric study for the baseline configuration and there was no effort to include additional noise reduction technologies. The system noise assessment reported here for the baseline configuration is for the aircraft as designed.

Table 1. Characteristics of Baseline Design

Parameter	Unit	Value
Maximum Takeoff Weight	lb	421826
Cruise Mach Number	-	0.85
Wing Span	ft	214.8
Wing Aspect Ratio	-	11.52
Wing Area	ft^2	4002.3
Reference Thrust	lb	112200
Engine Type	-	Turbofan
Number of Engines	-	2
Engine Diameter D	in	99
Engine Bypass Ratio	-	13.5
Engine Fan Pressure Ratio	-	1.6

Table 2. Design Features with Acoustic Benefits

Design Feature	Noise Reduction	Mechanism
Double-Deck Fuselage	Engine Noise at Sideline	Shielding
Advanced Wing	Airframe Noise at Approach	Low Flight Speed
Continuous Flap	Flap Noise	Reduce Side Edge Flow
Krueger Slat	Slat Cove Noise	Reduce Cove Flow Separation
High BPR Engine	Jet Noise	Low Exhaust Velocity
Advanced Liner	Fan Noise	Liner Absorption
Fuselage Mounting	Engine Noise at Sideline	Shielding and No Reflection
Behind Wing Mounting	Inlet Fan Noise	Shielding

Care must also be exercised in defining and selecting technologies for noise reduction. In the past two decades, there has been extensive research in developing noise reduction technologies for airframe noise components, including concepts such as cove filler and sealed gap for slats (Refs 8-10), fences, porous surfaces and continuous mold line for flap side edges (Refs 11-13), and fairings of various kinds for landing gears (Refs 14-16). None of the concepts, however, have made its way to current production aircraft. These issues have been considered in selecting technologies and design features for the baseline configuration in Table 2 as compared to the additional suite of noise reduction technologies assessed later.

In aircraft system noise assessment, flight operational conditions play an important role, because the flight parameters such as the flight Mach number and the aircraft angle of attack determine the noise source levels and the flight path determines the distance of the noise propagation, and hence, the amplitude of the noise received at the measurement locations. Similarly to aircraft design, flight procedures must also follow practical requirements, set by regulatory rules for safety and/or by airport authorities for operation efficiency. For example, current airport practice requires an aircraft to approach for landing at 3 degrees of flight path. Following rules such as this, the flight profile for the baseline configuration is designed and illustrated in Figure 2 for all three conditions of aircraft noise certification, plotting the flight altitude as a function of the touchdown distance. The three noise certification conditions are all shown in the figures as conventionally done; the first segment represents the approach condition with decreasing altitude, the short second segment is for ground operation, the third segment with increasing altitude represents normal takeoff when the sideline noise is measured, and the fourth segment is for engine power cutback operations with reduced climb rate.

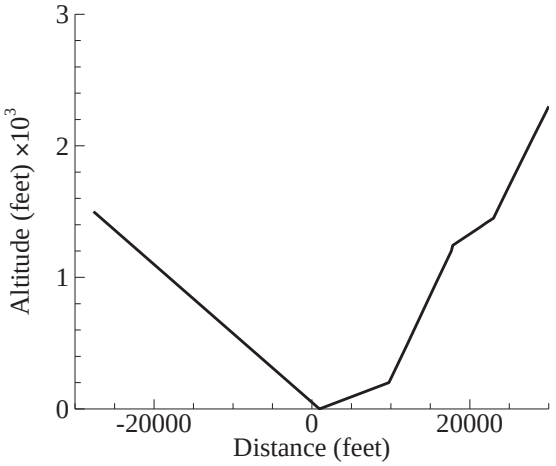

Figure 2. Flight profile for aircraft acoustic analysis.

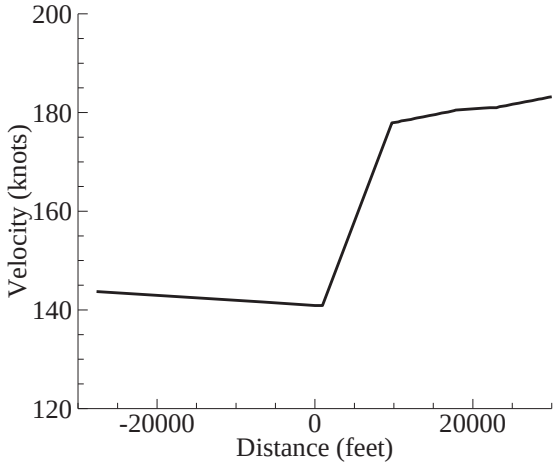

Figure 3. Flight velocity for aircraft acoustic analysis.

Similarly, Figure 3 plots the flight velocities along the flight path. Because of the efficient high lift wing design, the aircraft can land at speeds lower than typical landing speed for the current generation of aircraft of comparable size and functionality, by as much as 20 knots. This reduces the overall airframe noise because all airframe noise components scale on the flight speed, by either the six or the fifth power law. The 20 knots speed reduction corresponds approximately to a 3 dB reduction in airframe noise. The efficient high lift wing also helps reduce main landing gear noise by lowering the local flow velocity at the gear installation locations. This is due to the wing's large sectional lift, which induces a large circulatory flow under the wing in the opposite direction to the mean flow so that the total velocity under the wing is reduced. The flight conditions are also summarized in Table 3. In addition

to the flight profile and speed, the aircraft angle of attack and the total thrust is also shown in the table for all three aircraft noise certification conditions. The values of the total thrust illustrate the effects of efficient wing design. Because of the efficient lift generation, the engine thrust at approach conditions is only about 16 percent of the sideline power, and only 54 percent at cutback conditions.

Table 3. Flight Parameters at Noise Certification Conditions

	Approach	Cutback	Sideline
Altitude (ft)	400	2099	1000
Speed (knot)	141.6	180.9	179.9
AOA (deg)	3.1	5.4	5.1
Thrust (lb)	14864	49068	90330

III. Acoustic Analysis Methodology

The acoustic analysis methodology follows that in Refs 1, 7, and 17 that use a hybrid framework for aircraft system noise studies with individual elements in the framework assembled from various methods. While there are commonly used and validated tools for system noise assessment of conventional aircraft configurations, such as the NASA tool package Aircraft Noise Prediction Program (ANOPP) and the Boeing in-house tool Modular Component Prediction (MCP), acoustic tools directly applicable for advanced aircraft configurations such as the fuselage mounted engines studied here are still in the development stage. Predictions of turbofan engine noise for high bypass ratio engines currently rely heavily on very limited data with strong empirical nature, and the empirical engine noise tools are mostly stand-alone and are not incorporated in system noise assessment tools. For the shielding of engine noise, though much effort has been made to develop prediction tools in recent years, these tools are largely not available for system noise assessment. Some of methods are yet to be validated sufficiently and others are limited by their heavy computational resource requirements. Thus, noise shielding for full configuration aircraft can only be dealt with on an empirical basis by utilizing wind tunnel test data and implemented as a stand-alone process as part of the system noise prediction tool package.

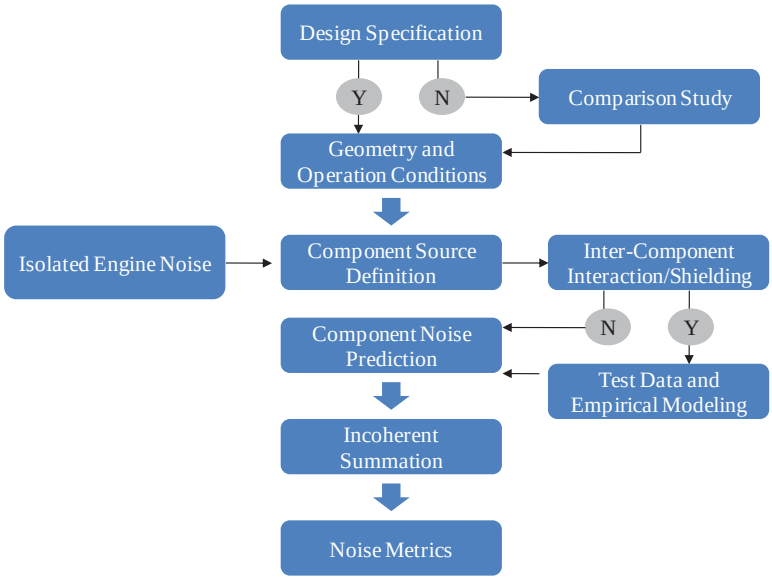

Figure 4. Illustration of acoustic analysis process.

Thus, it is of interest to describe the process used in the study presented here for system noise analysis, which is a combination of empirical prediction, component modeling and local feature numerical computation. The process is illustrated in Figure 4, consisting of the following elements. The acoustic analysis process starts with the design specifications, including the design of the airframe structure, engine type and power setting, and flight profiles. The design specifications are the basis for the noise component source level analysis for both the propulsion system and the airframe structure, and the flight profiles determine the operation conditions at the noise certification points.

From the aircraft design, propulsion system definitions are used to establish the engine noise source levels for all major engine noise components. For turbofan engines, they contain jet noise, core noise, forward fan noise and aft fan noise. The latter two are further decomposed into tonal noise and broadband noise. The component source levels also include those of the airframe structures, namely, the landing gears, the leading edge slats, the flap side edges and the trailing edges. The component noise source levels are for individual, isolated components, which need to be assembled under the constraints of the particular aircraft configuration to take into account of the inter-component interactions and shielding. This is a major feature of the advanced configuration where the engine noise may be significantly shielded by the airframe structure, effectively reducing the effects of source levels on the far field radiation. The far field noise from all the components is assembled into the total aircraft noise on an energy basis, meaning that the acoustic energies from all the components are summed together incoherently without considering the potential acoustic interactions between the components in the far field. The far field total noise levels are then used to compute the standard noise metrics, such as the Tone Corrected Perceived Noise Level (PNLT) and the Effective Perceived Noise Level (EPNL).

In the acoustic analysis procedure described above, the predictions of the airframe noise components, namely, the leading edge slats, the landing gears, the flap side edges and the trailing edge elevons, are based on methodologies developed for airframe noise components of conventional aircraft (Refs 18-24). These prediction models can be applied here for the advanced design because the basic elements of the prediction methodologies, such as the spectral features, the Mach number dependence, and the far field directivity of the radiated noise, are based on the fundamental theory of aerodynamic sound generation that captures the flow physics. The predictions are all component-based, with the noise prediction as a function of the local features of the individual components, rather than the overall design of the aircraft. The validation and calibration of the prediction models are also done for the individual components, and are not anchored on any particular aircraft type. This allows the models to have wide and robust applications.

The prediction of engine noise is another critical element in the acoustic analysis methodology. In addition to the prediction of the isolated noise source levels of advanced turbofan engines, the effects of the airframe on the engine noise must be accurately and realistically accounted for. The engine noise reduction due to shielding is the main factor that makes this advanced aircraft configuration acoustically advantageous compared to other design concepts as a candidate for future commercial aircraft. The engine noise source levels, including the tones and the broadband components, are predicted by empirical methods, calibrated by the data reported in Ref 1. Due to the lack of full scale engine noise tests and database for bypass ratios up to 14, especially for more advanced designs developed in recent years, the predictions can only be calibrated with limited model scale wind tunnel test data. The projection of the predictions to full scale, however, has shown good consistency with other independent methods and database.

The engine installation effects or airframe shielding effects include the shielding of inlet fan noise by the wings and the reflection and shielding of all engine noise components by the fuselage, especially at sideline conditions. Because of the advanced airframe and engine designs, there is no complete database available that can suitably account for all the installation effects for this aircraft. Thus, various methods and datasets will be used for the various engine noise components. For jet noise shielding by the fuselage, an empirical model will be used to account for the double deck fuselage. For core noise and fan noise shielding, datasets will be extracted from a wind tunnel test in the Boeing Low Speed Aeroacoustics Facility (LSAF), using simulated engine sources and a preexisting airframe model and will be discussed in detail in a later section.

IV. Engine Noise Shielding

In the past few years, a series of Propulsion Airframe Aeroacoustic (PAA) interaction effects tests have been conducted in Boeing's LSAF with a hot jet simulator for engine exhaust jet noise, broadband noise sources for engine core noise, and turbine powered open rotor model (Refs 6, 25-26). These tests had the objective of understanding the noise shielding characteristics with various combinations of airframes and noise sources. The shielding data from these tests, however, are not directly applicable to the aircraft configuration studied here. For example, there are no data for ducted tonal noise shielding which would be suitable for simulating the high bypass ratio turbofan tone noise. Even in cases where the wind tunnel test data can be used, the data are mostly for individual noise components, not for the total or overall engine noise. Thus, the engine noise shielding for the aircraft studied here will be accounted for by various datasets for the individual components, which is also a reflection of the multiplicity of engine noise sources and the different shielding effects experienced by the noise components for advanced aircraft configurations with high levels of airframe/engine integration. This will be discussed in detail in this section and is summarized in Table 4.

Table 4. Data Sources for Shielding Effects of Engine Noise Components

Component	Data
Core	Ducted Broadband Source Test
Jet in Flyover Plane	Jet Simulator Test
Jet at Sideline	Jet Simulator Test and Empirical Model
Forward Fan Tone	Open Rotor Interaction Tone at TE
Aft Fan Tone	Open Rotor Interaction Tone 1*D* Behind TE
Forward Fan Broadband	Ducted Broadband Source Test
Aft Fan Broadband	Ducted Broadband Source Test

When the wind tunnel test data are used for the shielding effects for the individual components, the overall conditions of the engine and aircraft operations and the noise measurements are matched, some directly, some by scaling laws, and some by interpolation. Parameters for direct matching, whenever applicable, include the mean flow Mach number, the aircraft angle of attack, the engine or noise source location, and the engine bypass ratio. Other parameters are matched by scaling laws based on frequency, engine power setting and fan rotational speed. The noise measurement angles are examples of interpolation; the measurement angles in the wind tunnel usually need to be corrected for flow effects and then interpolated to the far field angles in full configurations.

As can be seen from Table 4, the LSAF wind tunnel tests can provide shielding data for the jet noise component in the flyover plane, namely, for the approach and cutback conditions, but not for sideline conditions because the tests did not include sideline measurements on the shielded side of the aircraft fuselage due to limitations of the test facility. The test setup is illustrated in Figure 5, showing the LSAF test section, an airframe model and the jet simulator rig. For jet noise shielding in the flyover plane, Figure 6 plots the noise reduction due to shielding, namely, the difference in SPL between installed engines and isolated engines, as a function of polar emission angle and frequency, extrapolated to full scale frequencies. Positive values indicate noise increase and negative values are for noise reduction. It can be seen from the figure that jet noise shielding in the flyover plane is confined to the high frequency domain above about 2000 Hz, and the amount of noise reduction is small, on the order of 3 dB. At frequencies below about 2000 Hz, there is a slight noise increase on the order of one to two dB, essentially for all the emission angles. The lack of shielding is because the jet noise sources are distributed in the jet flow behind the engine nozzle, and thus, far away from the wings that are the shielding surfaces, while the noise increase is due to the reflection by the fuselage, which direct some acoustic waves to the flyover plane.

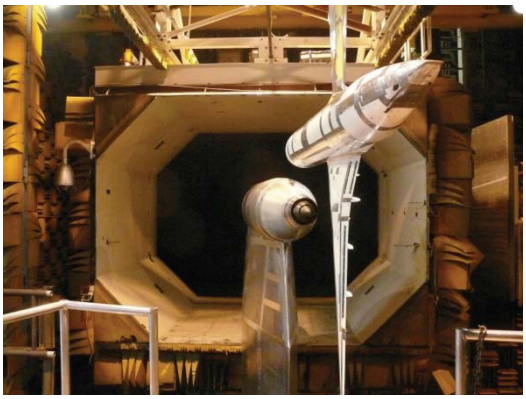

Figure 5. Test setup for the jet noise shielding test in LSAF.

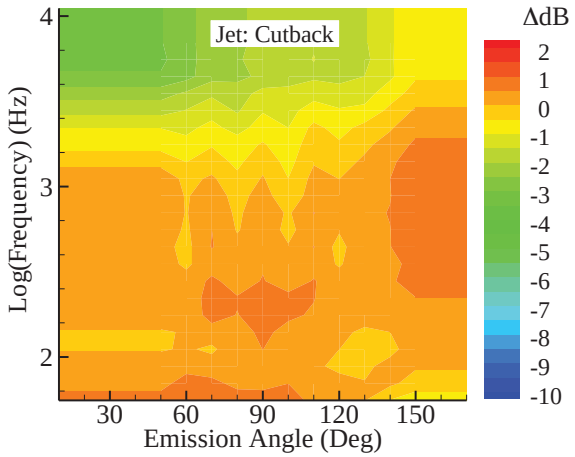

Figure 6. Shielding effects on jet noise in flyover plane with the jet at cutback power condition for full-scale frequencies.

Because of the size limitation of the test facility, the sideline microphones are located on the same side of the fuselage as the engine in the wing tunnel tests. Thus, the measurements include the effects of the fuselage reflection in the sideline direction, but not its shielding effects. To rectify this, a simple empirical model is added to the data to account for the shielding effects due to the fuselage, which is plotted in Figure 7 in terms of the difference in SPL due to the fuselage shielding as a function of the polar emission angle, with negative values for noise reduction. The empirical model considers the double deck fuselage as a perfect sound barrier for waves propagating in the forward quadrant, and hence, the 3 dB jet noise reduction to eliminate the noise from one of the two engines. The shielding becomes less efficient in the aft quadrant because the jet noise sources grow in size along the jet flow plume that may stretch behind the fuselage; the noise reduction gradually reduces to zero with increasing emission angle. This model is combined with the LSAF test data so that both the shielding and the reflection effects of the fuselage are accounted for in the sideline direction. The total installation effects on the jet noise component due to this combined effect are shown in Figure 8. It is clear that the overall acoustic effects of the fuselage mounted engines are beneficial; there is a noise reduction at all frequencies and in all emission angles, except for the low to intermediate frequency noise that escapes to the very large emission angles in the downstream direction.

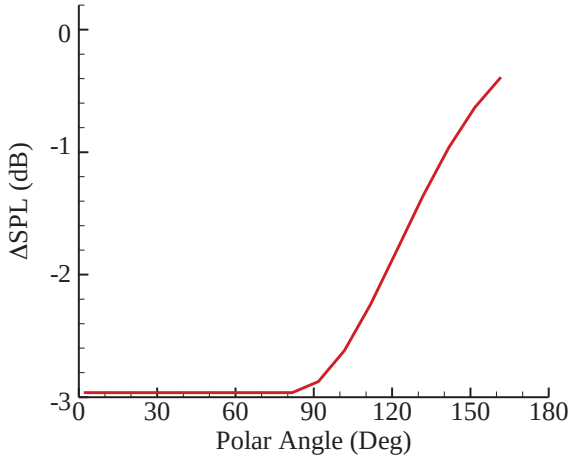

Figure 7. Fuselage shielding on engine jet noise in sideline direction.

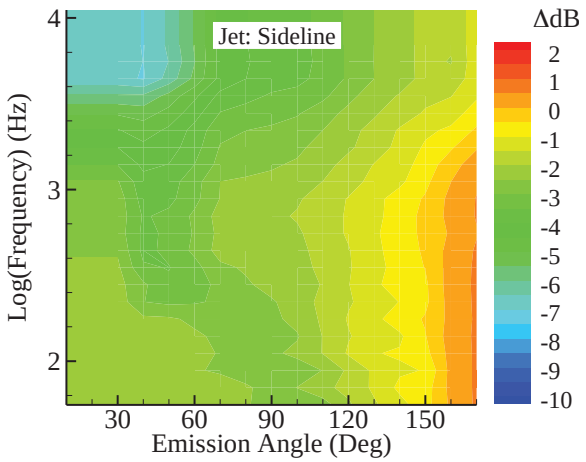

Figure 8. Total installation effects on jet noise due to fuselage shielding and reflection for full-scale frequencies.

The shielding effects to be applied to engine core noise sources are shown in Figure 9 and Figure 10, for both the flyover plane and the sideline direction. It is clear that significant shielding is provided by the wing in the forward quadrant. The amount of noise reduction increases with frequency, and shows interference patterns at low frequencies below about 800 Hz. This is a typical feature of sound scattering and diffraction where the direct radiation from the sources and the scattered/diffracted field interfere to form frequency dependent patterns. In the aft quadrant, there is a slight increase in noise levels, on the order of one to two dB, for the flyover plane shown in Figure 9. This is expected because there is no airframe structure to shield the core noise propagating out of the engine exhaust in the aft quadrant. Instead, the fuselage causes some reflection to enhance the noise levels in the flyover plane. While this noise increase due to fuselage reflection also affects the sideline direction, the increase is offset by the noise reduction due to the shielding of the noise from the engine on the other side, similar to the installation effects of the jet noise component. This explains Figure 10 where there is an overall noise reduction even in the aft quadrant.

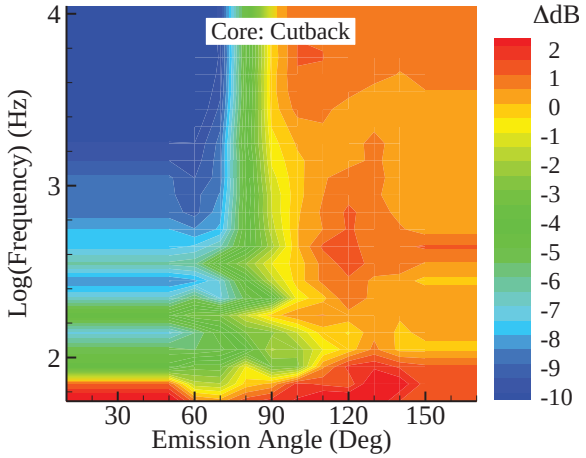

Figure 9. Shielding effects on engine core noise in flyover plane for full-scale frequencies.

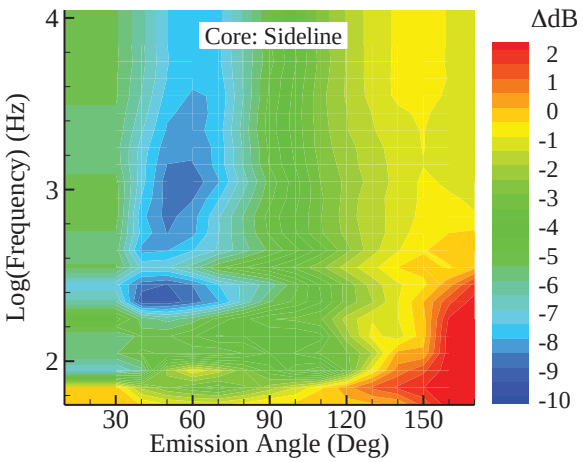

Figure 10. Shielding effects on engine core noise in sideline direction for full-scale frequencies.

Due to the high bypass ratio of the advanced direct-drive engine, tonal noise from the fan is a major component of the engine noise. As discussed in Refs 27-28 the application of the noise shielding effects from a wind tunnel test to full scale engines for tonal noise needs to be on the individual tones, which is different from the case of engines dominated by broadband jet noise, where the noise shielding is usually applied on the 1/3 octave band spectra, once the power settings are matched between the full scale engines and the scaled-up wind tunnel test engines. This is because engines dominated by jet noise follow similar acoustic behavior that is in turn mostly dominated by the engine power settings. On the other hand, the acoustic characteristics of large bypass ratio engines, their fan tonal frequencies, the tone amplitude distributions, and the directivities of the tones, are critically determined by the detailed designs and operating conditions of the fans. Thus, there is no guarantee for matching acoustic characteristics between two different designs, even if they can be operated to have the same power outputs. Of course, if the engines in the wind tunnel test have the same design as the full scale engine, the acoustic features of the two would be scalable and the shielding effects can be applied on the 1/3 octave band spectra. This is, however, not likely to be the case in practical situations, especially when the technologies of high bypass ratio engine design are still in development. Instead, less costly wind tunnel tests may be done using a generic engine design and the results should be suitably processed and applied to various full configuration designs. In this approach, the wind tunnel test serves, among other reasons, as realistic tone generators to gather shielding data at the individual tone frequencies. The shielding effects on the individual tones are relevant to other engines as long as the directivities of the tones individually match those of the tones in the full scale engines, even if the overall acoustic characteristics of the two are different.

Table 5. Turbofan Engine Tone Characteristics and Matching with LSAF Database

Engine Tone Characteristic	LSAF Open Rotor	LSAF Broadband Source	LSAF Jet Simulator
Spatial Distribution	Yes	No	No
High Coherence	Yes	No	No
Fwd/Aft Radiation	Yes	Yes	No
Engine Casing	No	Yes	No

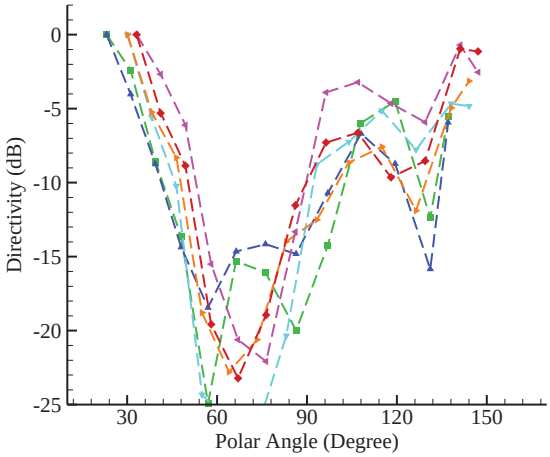

Figure 11 Directivities of the first interaction tones at takeoff power settings.

The tonal matching approach for fan noise shielding becomes even more necessary in this study because of the lack of data available for turbofan tone noise shielding. The study then calls for an approximate match of the source characteristics between the full scale engine and the wind tunnel test database, and the selection of subsets from the database that can best represent the shielding effects of turbofan engine tones. This is illustrated in Table 5, which lists in the first column the four major features of the tone noise sources for the high bypass ratio engines, namely, the source spatial distribution in the fan face, the high coherence of the sources, the directivity that radiates more in the forward and aft direction, and the engine casing that encloses the sources. The rest of the columns in the table list the three LSAF test databases. Apparently, none of them matches all the four major features of the turbofan tonal sources, and the open rotor database seems to be the best approximation. The fan face source distribution and the source coherence are similar between the two. The directivity of the turbofan tones can be matched by the interaction tones of the open rotor engines. The lack of engine casing that encloses the fan can also be rectified by only choosing the interaction tones from the open rotor database because this group of tones has directivity patterns that are similar to that of turbofan tone with maximum radiation in the forward and aft direction and minimum in between around the direction of the fan face plane. To illustrate Figure 11 plots the directivities of the first interaction tone at typical sideline power setting for aircraft takeoff operations. The results in the figure cover various parameters with the variations indicated by the different symbols, but the main feature is that the directivity pattern which is very similar to that of turbofan tones. Thus, the shielding effects of these tones can be expected to be a good approximation for the turbofan tones.

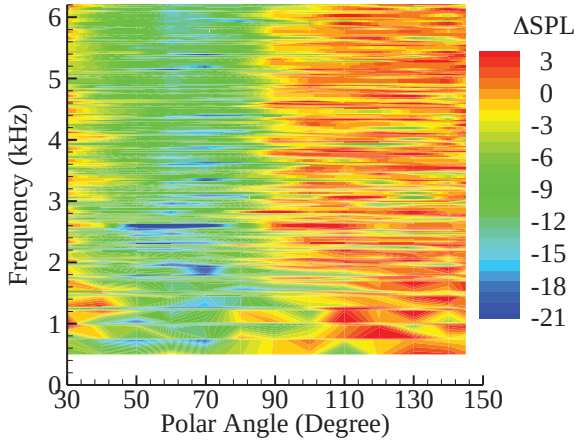

Figure 12. Forward fan noise shielding in flyover plane for full-scale frequencies.

The shielding effects of the wing on forward fan tonal noise is illustrated in Figure 12, which plots the difference in SPL between installed and isolated engine noise as a function of polar emission angle and frequency. The data are

extracted from the LSAF database for open rotors, selecting only interactions tones. The test conditions are typical of aircraft takeoff operations and the emission angles are in the flyover plane. Since the engine inlet lip is aligned with the wing trailing edge, noise radiating to the forward quadrant is significantly shielded; within the angular domain from about 30 to 90 degrees, noise reduction can be as high as 20 dB and on average about 10 dB. At small emission angles below about 30 degrees, shielding is less efficient because the finite chord length of the wing lets some noise propagate directly to the far field, as expected from the principles of geometric acoustics (Refs 29-30). It can be seen from the figure that there is a slight noise increase in the aft quadrant for emission angles larger than 90 degrees, on average between one and two dB. This noise increase is due to the fuselage reflection, again explainable by geometric acoustics; for engines installed close to the fuselage, some sound waves from the engine can be reflected by the fuselage to reach the far field below the engine, in addition to the direct radiation that would be the only noise component for isolated engines. This also applies to jet and core noise, as discussed early in this section and shown in Figure 6 and Figure 9.

The engine installation effects at sideline locations include not only the wing shielding and the fuselage reflection, but also fuselage shielding when the measurements and the engine are on opposite sides of the fuselage. This is illustrated in Figure 13 and Figure 14, for far field locations respectively on the same side as the engine and on the opposite side to the engine. For the former, the shielding features are similar to that in the flyover plane, except for the smaller amount of noise reduction in the shielded zone and the less clearly defined boundaries of the shielded zone. Both of these are due to the wing tapering and sweeping, leading to a smaller effective chord length for shielding. For the case where the far field location is on the opposite side of the fuselage, shown in Figure 14, the fuselage provides significant shielding in the sideline direction so that noise reduction is seen in almost all the emission angles. The noise reduction is more than 10 dB in the forward quadrant and becomes less as the emission angle increases, which is also the feature modeled in Figure 7 for jet noise, assuming complete blocking out in the forward quadrant and less efficient shielding in the aft quadrant.

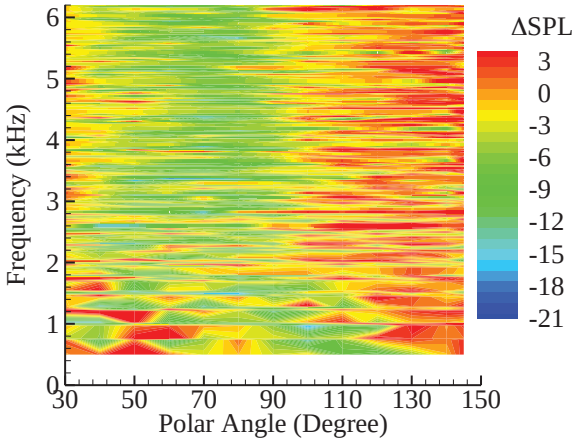

Figure 13. Forward fan noise shielding at sideline on the same side as engine source for full-scale frequencies.

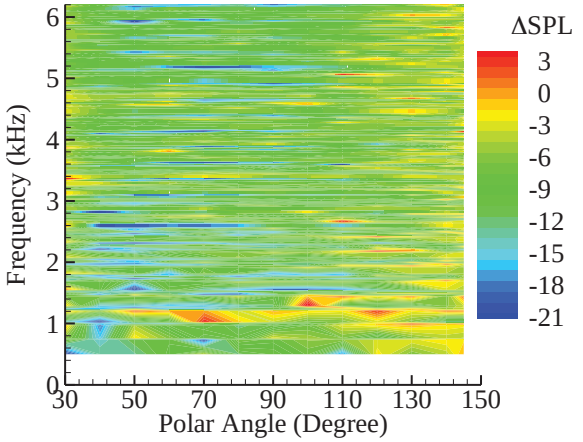

Figure 14. Forward fan noise shielding at sideline on opposite side to engine source for full-scale frequencies.

For the aft fan tones mostly propagating in the downstream direction, the shielding and reflection due to the wing and fuselage are similar to the forward fan tones, except for the much smaller wing shielding benefit because the engine nozzle from which the aft fan noise radiates is further away from the wing trailing edge. This can be seen from Figure 15 which plots the shielding effects for the aft fan tones in the flyover plane, again, for typical aircraft takeoff operations. As expected, the shielding zone is shifted in the upstream direction, to angles below about 50 degrees, and the amount of noise reduction in the shielded zone becomes small, on the order of about 5 dB. This is, however, not a drawback for practical applications, because the aft fan noise mostly radiates in the downstream direction in the aft quadrant, and thus, the amount of reduction in the forward quadrant is less relevant. On the other hand, the increase in noise levels in the aft quadrant for the flyover plane may have a direct adverse impact on the total aircraft noise. This is a disadvantage of the fuselage mounted engines and is more of a practical concern especially for large bypass ratio engines whose noise is dominated by fan tones.

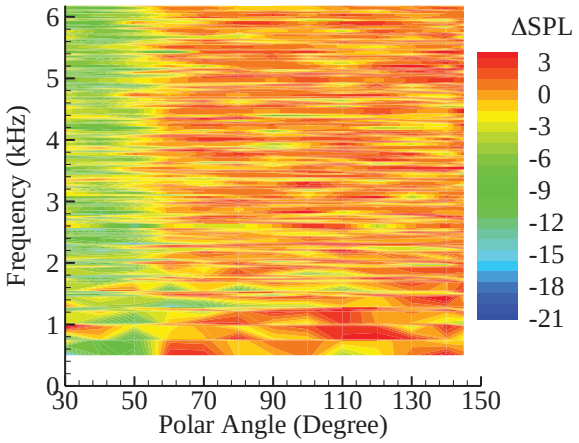

Figure 15. Aft fan noise shielding in flyover plane for full-scale frequencies.

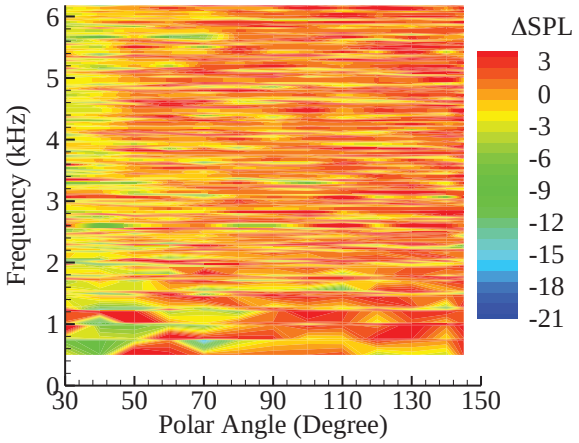

Figure 16. Aft fan noise shielding in sideline direction on the same side as engine source for full-scale frequencies.

For aft fan noise in the sideline direction, the effects of the wing is minimum and the installation effects are dominated by the fuselage reflection and shielding, respectively for the far field location on the same side and on the opposite side of the fuselage, which are illustrated in Figure 16 and Figure 17. When the far field is on the same side as the engine, Figure 16 shows that the effects of the airframe is essentially a noise increase, almost uniformly in emission angle and frequency due to the fuselage reflection. When the far field is on the opposite side to the engine, however, the effects are essentially a uniform noise reduction, due to fuselage shielding plotted in Figure 17.

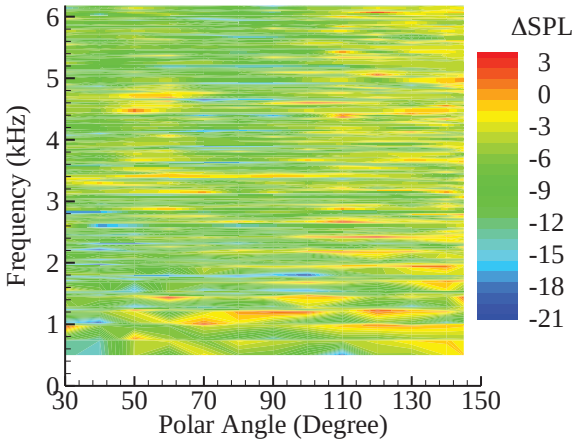

Figure 17. Aft fan noise shielding in sideline direction on opposite side to engine source for full-scale frequencies.

V. System Noise Results of Baseline Configuration

The system noise study starts with the baseline configuration with both the propulsion system and the airframe configuration as designed, details of which are described in Section II and in Ref 1. The configuration includes inherent technology that will lower noise and the design does follow some general principles to minimize noise, but there is no specific acoustic optimization or parametric studies. Instead, the configuration is designed to meet aerodynamic and propulsion requirements. Thus, the acoustic analysis serves only as an assessment of the as-designed configuration. An example is the engine design and the installation positions. While the use of large bypass ratio engines helps reducing the engine noise source levels and the fuselage mounting above the wings provides some shielding, neither has been optimized for noise. One reason for focusing first on the acoustic assessment of the baseline configuration is to highlight the design that is considered to be most practically feasible within the 2025 timeframe. Another reason for the baseline acoustic analysis is to demonstrate the multiple paths to achieve further noise reduction goals. With the baseline configuration as the starting point, further noise reduction can be projected from various combinations of approaches and this will be presented in Sections VI and VIII.

With the methodologies and data described in the previous sections, the noise metrics for the baseline configuration are calculated and summarized in Table 6, which lists the limits of the noise regulation of Stage 3 at the three certification conditions and their cumulative value as the first row of data in the table. The EPNL for the advanced aircraft is then given in the second row, which leads to the margins given in the next two rows respectively in reference to the regulation limits of Stage 3 and Stage 4, the latter being the current regulation for aircraft certification. Clearly, this is a quiet aircraft, with about 28 dB cumulative EPNL margin to Stage 4. As a reference comparison, the latest generation of commercial aircraft currently in service, the Boeing 787, for example, which has the conventional design with turbofan engines and has comparable takeoff weight to the configuration studied here, has cumulative EPNL of about 17 dB below Stage 4.

Table 6. Acoustic Results for the Baseline Configuration

	Approach	Cutback	Sideline	CUM
Stage 3 EPNL Limits (dB)	104.0	97.4	100.6	302.0
EPNL (dB)	91.1	86.0	86.9	264.0
Margin to Stage 3 (dB)	12.9	11.4	13.7	38.0
Margin to Stage 4 (dB)	-	-	-	28.0

The low noise levels of the aircraft are achieved by the advanced wing design, allowing low approach speed, the large bypass ratio engines, lowering the engine noise source levels, and the shielding of engine noise by the airframe structure, reducing the noise propagating to the far field. The engine installation effects include both shielding and reflection, and can be demonstrated by a reference comparison between the baseline design and a hypothetical aircraft that uses the same engines, but does not provide any engine noise shielding and reflection. To be relevant,

the hypothetical aircraft is assumed to have the same levels of airframe noise components as the baseline aircraft. It is also assumed to operate with the same flight profiles. The noise levels of this hypothetical aircraft are compared with the baseline aircraft in Table 7, showing the aggregate effects of the wing shielding, fuselage shielding and fuselage reflection, with noise reduction of 0.8, 0.7 and 2.6 dB, respectively for the approach, the cutback and the sideline condition. From Table 7, it can be seen that though the installation effects provide a total of 4.1 dB to the comfortable EPNL margin of the baseline configuration, the advanced engine and airframe design also has good acoustic characteristics. Even without the shielding, the hypothetic aircraft would still meet the regulatory noise requirements, with an EPNL margin of about 24 dB. It should be pointed out that this hypothetical aircraft is used here only to demonstrate the effects of engine installation from shielding. It is by no means an indication of the noise levels for conventional aircraft designs, which have drastically different airframes, and thus, very different airframe noise levels. Because of the differences in airframe design, conventional aircraft also operates with flight profiles different from those of the aircraft studied here, such as the flight Mach number. Furthermore, for engines installed under the wings of conventional aircraft designs, the wing reflection would also have a significant effect on the total aircraft noise. Therefore, the difference between this baseline aircraft and an equivalent engine-under-the-wing configuration would likely be more than the 4.1 EPNLdB, cumulative.

Table 7. Comparison between the Baseline and a Hypothetical Aircraft without Shielding.

	Approach	Cutback	Sideline	CUM
Stage 3 EPNL Limits (dB)	104.0	97.4	100.6	302.0
EPNL (dB)	91.1	86.0	86.9	264.0
Hypothetical Aircraft EPNL (dB)	91.9	86.7	89.5	268.1
Shielding Effect (ΔdB)	0.8	0.7	2.6	4.1

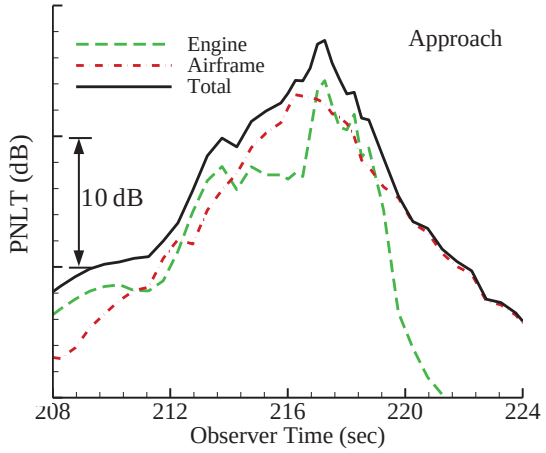

Figure 18. PNLT for the baseline configuration at approach conditions.

The combination of advanced engine design and shielding is so efficient in reducing the engine noise at approach conditions that the engine noise is no longer the clearly dominant component. This can be seen from the component decomposition shown in Figure 18, which plots the tone corrected perceived noise level (PNLT) as a function of the observer time for both the airframe and the engine noise component, as well as the total, at the approach condition. In this case, the engine noise, indicated by the green dashed line, still has noticeable contributions in the aft quadrant at observer times after the peak noise point in the diagram, but the dominant component elsewhere is the airframe, shown by the red curve in the figure. Similarly, Figure 19 and Figure 20 plot the noise decomposition in PNLT respectively for the cutback and the sideline certification conditions. It can be seen that for all three conditions, the engine noise components are significantly reduced in the forward quadrant, namely, at observer times before the peak noise time in the figure when the observer is ahead of the aircraft. The engine noise levels are much lower on the left side of the peak noise points, compared with the levels on the right side. This is expected because the engines are located close to the trailing edges of the wings so that most shielding occurs in the forward directions. The figures also show that the engine noise even after shielding is still a major contributor to the total aircraft noise, especially in the aft quadrant. This is true for all three conditions, but especially at sideline and cutback.

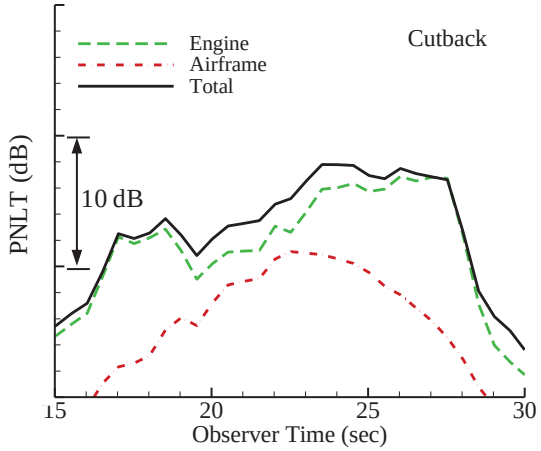

Figure 19. PNLT for the baseline configuration at the cutback condition.

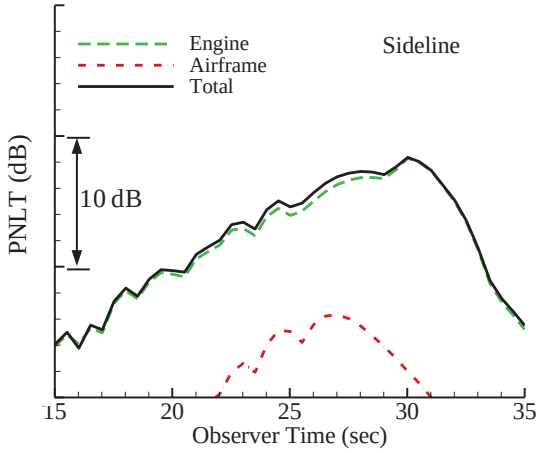

Figure 20. PNLT for the baseline configuration at the sideline condition.

For the approach conditions when the airframe is the major contributor to the aircraft total noise, the noise decomposition can be carried out further for all the airframe noise components, as shown in Figure 21, where the main landing gears, the flap side edges and the slats are seen to be the major noise components. It should be pointed out that the slats in the configuration studied here are Krueger slats, designed for the purpose of implementing and protecting laminar flow control devices around the leading edge of the wing. The prediction of Krueger slats is based on conventional slotted slats and regards the effects of the Krueger design as being similar to cove fillers because both reduce or suppress the flow separation in the cove region. Because of the structural design and implementation mechanism of Kruger slats, a series of brackets along the wing span are used to support and deploy the slats, which can be a new noise component. This has not been studied and it is not known how much contribution this new noise component will make to the total aircraft noise. Currently, the noise from the slats themselves is considered to be much higher than that from the supporting brackets, so that the bracket noise is ignored in this analysis, similarly to other minor airframe noise components. For Krueger slats, the number of brackets and the complexity of the brackets may be very different from those for conventional slotted slats, which would then represent a new noise component.

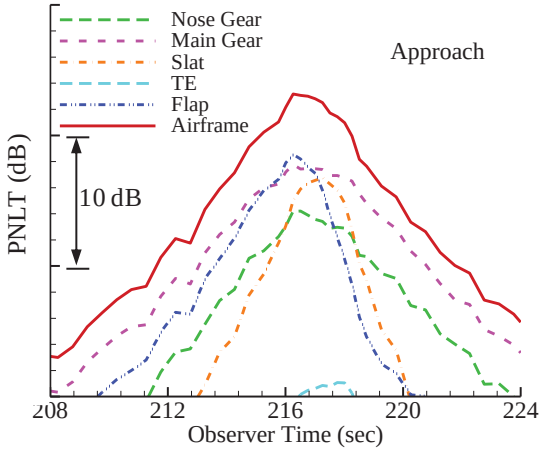

Figure 21. PNLT for airframe components only at approach condition.

VI. Noise Assessment of B27 with Noise Reduction Suite of Technologies

To study the potential for further noise reduction, various noise reduction concepts currently in research and development are considered in this section, both individually and collectively applied to the baseline configuration to quantify the acoustic benefit of each individual technology, as well as the aggregate impact on the aircraft system noise. The noise reduction concepts can be divided into engine noise reduction and airframe noise reduction. For engine noise reduction, the technologies are summarized in Table 8 with a brief description for each concept, the amount of noise reduction, the targeted noise components, the spectral and angular distribution of the reduction, and the sources of the data used in the system noise study. The concepts include over-the-rotor (OTR) and soft vane (SV) liner treatments for all fan-related noise components (Refs 31-32), an exhaust scarf nozzle with a 10 degree scarf angle that effectively shields aft fan noise and core noise, a low noise engine pylon for jet and fan noise (Ref 6), and a chevron nozzle that has proven successful in jet noise suppression (Refs 33-34). Similarly for airframe noise reduction, various concepts currently in development are summarized in Table 9, following the same format as that for engine noise reduction concepts. Included in the table are optimization of high lift wings that may allow a further reduction in aircraft approach speed, and hence, reduction in overall airframe noise, a sealed slat gap, which can eliminate/reduce slat noise source associated with the high speed gap flow (Refs 8-10), flap side edge treatments such as porous surfaces that reduce the rollup vortex at the flap side edges due to the edge cross flow (Refs 11-13), and landing gear fairing and redesign, which can either shield the gear parts from the incoming flow or smooth out the geometry to reduce flow separation (Refs 14-16).

The implementation of these concepts may involve add-on devices and/or design changes. Landing gear fairings and over the rotor and soft vane liner are examples of the former, while more efficient high lift wing design and scarf nozzle are examples of the latter. In both cases, the implementation can affect the aircraft design, in terms of the added weight, and hence, the extra fuel burn, and/or aerodynamic and propulsion changes. Thus, the implementation of noise reduction technologies should be an integral part of the aircraft design, to balance the various effects. In the fuel burn assessment, the weight impact of these technologies will be included. The quantification of the acoustic benefit and fuel burn impact of this suite of technologies can then serve as a starting point for future parametric studies in aircraft optimization.

For the baseline configuration considered earlier, slat noise reduction was considered in the form of the Krueger slats that was sealed for takeoff and open for approach. In this additional noise reduction approach, the gap is also sealed on approach, a design which would likely mature in the form of hinged Krueger slats without gaps. Or an active technology could also be feasible, sealing the slat gaps at normal operation conditions but opening up the gap at extreme conditions when maximum lift is required. These projected technologies make the slat noise very low, in comparison with other noise components, as will be seen in later sections, because the Krueger slats efficiently reduces the cove noise and the sealed gaps effectively eliminate the gap noise.

Technologies for reducing landing gear noise are also possible to mature enough for practical applications and to be available in the next 10 to 15 years, and thus considered here. The technologies may be in the form of local fairings, redesign of the gear parts or reconfiguration, and overall fairings, all of which have been actively researched in recent years. Though these concepts have all been shown to have acoustic benefits, the amount of reduction, however, scatters significantly in the reported results in the literature. In this study, we use a frequency-

dependent model for the noise reduction, accounting for the efficient reduction at frequencies for which the devices are designed and the less efficient or even noise increase at other frequencies. The reduction assumes maximum value of 5 dB at the peak frequency of the treated component and gradually tapers off on both sides of the peak frequency. The reduction is assumed to be efficient within a decade centered at the peak frequency.

Table 8. Engine Noise Reduction Technologies

Technology	SPL Reduction	Data Source
Over the Rotor & Soft Vane Liner	• Up to 4 dB for Full Success Implementation • Uniform in frequencies and emission angles • Applied to all fan noise components	NASA
Pylon	• Reduction amount from data • Frequency and angle dependent • Applied to jet noise	LSAF
Scarf Nozzle	• Reduction amount from data • Frequency and angle dependent • Nozzle long side in flyover plane • Applied to aft fan and core noise	LSAF
Chevron	• Amount from empirical data and modeling • Frequency and angle dependent • Applied to jet noise	Boeing

Table 9. Airframe Noise Reduction Technologies

Technology	SPL Reduction	Data Source
High Lift Wing Optimization	• Up to 10% approach speed reduction • AFN components reduction • Frequency and angle dependent	Prediction
Landing Gear Fairing	• Amount from empirical data and modeling • Local partial and full fairing • Frequency and angle dependent • Applied to both main and nose gear	Boeing
Porous Flap Side Edge	• Amount from empirical data and modeling • Frequency and angle dependent	Boeing
Sealed Slat Gap	• Amount from validated prediction • Uniform in frequency and angle • Applied to slat noise	Boeing

The noise reductions achieved from the advanced technologies are listed in Table 10, showing that these concepts have the potential to further reduce noise except for the pylon design. This is likely due to the high bypass ratio of the engine and the lessor impact of the jet component that is primarily impacted by the pylon design. To reveal the details of the acoustic impact of the technologies, the table lists the EPNL for all three certification conditions, as well as the cumulative levels, with the technologies applied to the baseline configuration. The cumulative EPNL is compared with the Stage 4 limits and the noise margins are given in the table. Comparisons are also made with the noise levels of the baseline configuration and the amounts of noise reduction from the baseline are given in the last column in the table. The rows in the table are for the individual technologies, except for the last row which is for all the technologies applied to the baseline, and hence, representing the aggregate effects of the entire suite of technologies.

Table 10. Acoustic Benefit of Advanced Noise Reduction Technology Suite

	Approach	Cutback	Sideline	CUM	Margin to Stage 4	Reduction From Baseline, dB
Baseline	91.1	86.0	86.9	264.0	28.0	-
OTR/SV	90.3	84.5	86.1	260.9	31.0	3.0
Pylon	91.1	86.0	86.9	264.0	28.0	0.0
Scarf Nozzle	90.8	85.6	86.9	263.3	28.6	0.7
Chevron	91.0	85.8	86.5	263.3	28.6	0.7
Wing Design	90.5	86.0	86.9	263.4	28.2	0.3
LG Fairing	90.6	86.0	86.9	263.5	28.4	0.5
Porous Flap SE	90.5	85.6	86.8	262.9	29.0	1.1
Sealed Slat Gap	90.9	86.0	86.9	263.8	28.1	0.2
All	87.4	83.4	85.2	256.0	35.9	8.0

From the table, it can be seen that the treatment of over the rotor and soft vane liner has the largest individual reduction, about 3 EPNL dB, as listed in the second row. This can be expected from the noise component decomposition discussed in the previous section, where it is shown that the engine aft fan noise is the major noise component, due to the lack of wing shielding and the reflection of the fuselage for this component. This treatment directly targets the fan noise, leading to the large noise reduction. It is shown in the table that the noise reduction is effective at all three certification condition, with reductions of 0.8, 1.5 and 0.7 dB respectively for the approach, cutback and sideline conditions. The largest reduction comes from the cutback conditions where aft fan noise is the dominant component, while the airframe noise and the jet noise hold up the reduction respectively for the approach and sideline conditions. The case shown in the table for this technology assumes a reduction of 4 dB in SPL uniformly for all frequencies and emission angles, applied to all fan noise components at all three certification conditions, which is considered to be an aggressive assumption, and thus, probably representing the upper bound of the noise reduction potential for this technology. It is also interesting to note that though a reduction in cumulative EPNL of 3 dB, or approximately 1 dB for each certification condition, is significant, it is achieved in this case by a much larger uniform reduction of 4 dB in SPL. This is a known feature of aircraft system noise; the noise metrics are determined not only by the balance of various individual components, but also by other factors such as the tonal nature of the components and the duration of the noise exposure. Thus, a promising concept for an individual noise component illustrated in component tests may not necessarily translate to comparable acoustic benefit for aircraft system noise.

This also applies to other noise reduction concepts listed in Table 10. Generally, the noise reduction for the individual components is on the order of a few dB for SPL, which usually leads to much smaller reductions in EPNL, depending on the ranking order of the noise components. An example in airframe noise is the technology of continuous mold line (CML) flaps that smoothes out the disruptive aerodynamic behavior of flap side edges, and thus, reducing flap side edge (SE) noise. In component wind tunnel tests with small scale and simplified flap models, it has been observed that the noise reduction is very effective, as much as 6 dB in SPL reduction. This large SPL reduction, however, only yields about 1.1 dB of cumulative EPNL reduction for this aircraft, because once the flap side edge noise is reduced to levels lower than other components, further reduction for this component would have less and less impact on the total noise, which is why the benefit of this technology is so limited for the aircraft studied here. In fact, Table 10 lists the porous flap side edge treatment as the technology applied to the flaps because while it only has about 3 dB of SPL reduction on the component basis, this is enough to produce the same system level benefit as continuous mold line technology and, furthermore, the porous side edge technology is the more likely to meet implementation criteria.

The results in Table 10 are derived by assuming fully successful implementation of the noise reduction technologies at levels most of which represent the upper bound of the acoustic benefits. When all the technologies are applied to the baseline configuration (with the BPR 13.5 engine), there is a potential of about 8 dB of additional noise reduction, bringing the cumulative EPNL of this aircraft to 36 dB below Stage 4. However, it is important to emphasize that this assumes that the whole suite of noise reduction technologies would all mature for practical applications in the next decade or so, a very challenging and aggressive assumption. It must be noted that some of

the concepts are only in their early stage of research, and some may not be feasible or favorable in aircraft design even when the technologies are mature, because of their potential adverse impact on aircraft performance.

VII. Fuel Burn Reduction of the B27 with GTF Engines and Noise Reduction Suite

A. Baseline Background

In addition to noise reduction, NASA's subsonic transport system level metrics include aircraft fuel/energy consumption reduction goals. For the N+2 timeframe, defined as a Technology Readiness Level of 4-6 by 2020, the current goal is a 50% fuel burn reduction relative to a 2005 best-in-class baseline. For the large twin aisle class, the 2005 best-in-class baseline is represented by the Boeing 777 with GE90 engines. This can be associated with a 1998 technology level, since the first 777 and its initial long range derivative (777-200ER) entered service in that timeframe.

The B27 concept emerged from a NASA sponsored, N+2 timeframe, advanced vehicle concept study (Ref 1). The baseline mission requirements provided by NASA for that study were very similar to estimates of the state-of-the-art performance capability of the Boeing 787-8. Since the current fuel burn metric is relative to a 2005 best-in-class capability, and the 787-8 entered service six years after that point, part of the study was to develop a 1998 technology level baseline concept. This concept utilized 777-200ER level technology assumptions applied to a 787-8 type mission of 8,000 nm range with a 50,000 lb payload and a cruise M=0.85. The estimated block fuel burn for this concept, referred to by Boeing as the "1998 T&W-0001", was 254,955 lb (Ref 1). Boeing then developed a series of advanced N+2 timeframe concepts, including the -0027A, a tube-and-wing with a T-tail mounted on the aft fuselage, a double-deck passenger cabin and twin podded engines on horizontal, fuselage-mounted pylons with the engine inlet lip located just forward of the wing trailing edge (Ref 1). This concept was estimated to have a 42% fuel burn reduction compared to the Boeing 1998 baseline design, and is the starting point for the current analysis effort.

B. Fuel Burn Assessment Methodology

This fuel burn assessment was performed using two separate approaches. The first approach utilized Boeing's 1998 baseline to calculate the fuel burn metric, the second approach utilized a NASA generated baseline design. The Boeing generated baseline utilized a "PW4090like" engine model, and the NASA generated design utilized a "GE90-94Blike" engine model. Table 11 shows relevant parameters for both baseline cases. The differences in the engine models and other assumptions between the two baselines resulted in significantly less fuel required for the sized (optimized for minimum fuel burn) NASA baseline design, enabling a smaller and lighter concept.

Table 11. Comparison of Boeing and NASA 1998 Baseline Designs

	Units	Boeing 1998 Baseline	NASA 1998 Baseline
Engine Model		PW4090like	GE90-94Blike
Takeoff Gross Weight	lb	624,154	534,698
Operating Empty Weight	lb	291,171	243,971
Payload	lb	50,000	50,000
Range	nm	8000	8000
Block Fuel	lb	254,955	218,637
Wing Area	ft2	5808	4562
Wing Span	ft	221.4	199.2
Wing Aspect Ratio		8.4	8.7
Wing Loading	lb/ft2	107.5	117.2
Max Thrust per Engine	lb	92,800	73,800
Cruise Mach #		0.85	0.85
Start of Cruise L/D		19.8	18.2

This also reduces the relative performance of the B27 concept due to the lower fuel burn of the baseline, which prompted the use of the two separate approaches in estimating the B27 fuel burn metric.

A FLOPS (Ref 35) model for the -0027A concept was created and calibrated to the Boeing data, and was used as the starting point for both analysis approaches. To construct the B27 concept, additional N+2 technologies in the noise and fuel burn areas were included resulting in a more aggressive N+2 concept in an attempt to assess the feasibility and associated technology path required to meet the NASA metrics. The additional noise technologies are presented above, in Section VI. The fuel burn impacts of these additional noise technologies were estimated as follows. The scarf nozzle is assumed to have a 0.1% thrust penalty and a weight equal to 5% of the baseline nacelle weight. The landing gear fairings were assumed to have a weight equal to 2% of the baseline gear weight. All other noise technologies were assumed to have a negligible impact on the overall configuration fuel burn performance. The wing aspect ratio was also increased, and a GTF engine model was sized for the configuration. While more aggressive compared to the -0027A in some areas, it is important to note that the technology assumptions of the B27 are similar to those of other N+2 concepts in the current peer group of NASA studies.

The Boeing study utilized a large variety of engine types, including both direct drive and geared architectures. The -0027A concept utilized a Rolls Royce direct drive engine concept with a BPR = 13.5. For the purposes of this fuel burn assessment, an N+2 timeframe GTF engine model with BPR = 15 was utilized. Table 12 presents relevant parameters for the uninstalled engine model, including a weight build-up and overall dimensions prior to scaling. Note the sea level static thrust of 72,050 lb is greater than the ~60,000 lb thrust required for the B27. Therefore, this engine was scaled down as part of the concept sizing process.

Table 12. N+2 GTF Uninstalled Engine Parameters

	Units	Sea Level Static	Top-of-Climb			
Mach		0	0.8	Bare Engine Weight	lb	14500
Altitude	ft	0	35,000	Accessories Weight	lb	1450
Thrust	lbf	72050	12430	Engine Mount Weight	lb	293
Specific Fuel Consumption	lb/(lbf hr)	0.2457	0.4773	Total Engine Weight	lb	16243
Overall Pressure Ratio		50.9	55.1	Inlet & Nacelle Weight	lb	1642
Bypass Ratio		14.05	14.9	Total Engine Pod Weight	lb	17885
Fan Pressure Ratio		1.36	1.375	Engine Pod Length (in)	in	237
				Nacelle Max Diam (in)	in	155

C. Fuel Burn Analysis Results

Starting with the calibrated -0027A FLOPS model, the changes listed in the above section were made and the model was sized allowing the engines to scale as needed. The active constraint for the engine sizing was the 300 ft/min rate of climb requirement at top-of-climb conditions. The required engine thrust was 60,100 lb per engine, resulting in an engine scale factor of 0.83. Table 13 presents a concept data summary for this model under the column heading, “FLOPS B27 Model Approach 1”. Utilizing the Boeing 1998 baseline concept block fuel burn of 254,956 lb, this concept is estimated to have a 47.5% fuel burn reduction.

Next, starting with the calibrated -0027A FLOPS model, the changes listed in the above section were made and the concept was sized again, however in this approach both the thrust and the wing area were optimized. Additionally, calibration factors utilized to match the Boeing data were reset to be consistent with the NASA 1998 baseline modeling approach, resulting in a more consistent basis for comparison. In this case, the wing was sized by the landing constraint of 5,200 ft, and the need to provide adequate fuel volume. The resulting wing reference area was 3,630 ft (Ref 35). The column labeled “FLOPS B27like Model Approach 2” in Table 13 contains the concept data summary for this approach. Utilizing the NASA 1998 baseline concept block fuel burn of 218,640 lb, this concept is estimated to have a 42.9% fuel burn reduction.

The two different baselines utilized for this fuel burn assessment enable comparisons to be made to concepts from similar studies with the appropriate baseline. For example, as part of the Boeing advanced vehicle concept study, Boeing developed another N+2 concept with very high bypass ratio GTF engines called the “BWB -0009A ”. Even though the engines are not exactly equivalent, the technology assumptions, mission requirements, and the Boeing 1998 baseline are very similar. The BWB -0009A fuel burn reduction was reported as 53.7% as compared to the 47.5% of the current B27.

Table 13. Fuel Burn Analysis Results

	Units	FLOPS B27 Model Approach 1	FLOPS B27like Model Approach 2
Takeoff Gross Weight	lb	437,600	405,500
Operating Empty Weight	lb	239,850	217,000
Payload	lb	50,000	50,000
Range	nm	8000	8000
Block Fuel	lb	133,850	124,930
Wing Area	ft2	4002	3630
Wing Span	ft	206.9	194.0
Wing Aspect Ratio (trap/gross)		13.9 / 10.7	13.9 / 10.4
Wing Loading	lb/ft2	109.3	111.7
Max Thrust per Engine	lb	60,100	64,500
Engine Scale Factor		0.83	0.90
Cruise Mach #		0.85	0.85
Start of Cruise L/D		23.1	23.3
Start of Cruise SFC	lb/(lbf hr)	0.49	0.49
Boeing 1998 Baseline Block Fuel	lb	254,956	218,637
Fuel Burn Reduction		47.5%	42.9%

VIII. Noise Projection of B27 with GTF Engine and Noise Reduction Suite

To this point in this study, a noise assessment has been performed in Section VI on the baseline B27 configuration with the BPR 13.5 direct drive turbofan and then a second assessment with a suite of noise reduction technologies added. In Section VII the fuel burn assessment was presented on the B27 with the same suite of noise reduction technologies but with a higher bypass ratio, approximately 15, GTF engine with a lower fan pressure ratio as compared to the direct drive turbofan.

For engine technology, the direct drive bypass ratio of 13.5 engine is expected to be feasible for practical application in about 10 years or so, but it is not considered the technology limit in the N+2 timeframe. Advanced design technologies may allow even higher bypass ratio engines resulting in lower engine source noise levels. Indeed, in the study reported in Ref 1, a design of a Geared Turbofan engine with a bypass ratio of 18, fan pressure ratio (FPR) of 1.25, was also considered in the same N+2 timeframe for a Blended-Wing-Body (BWB) aircraft. This BWB aircraft was assessed at 41.6 dB cumulative below Stage 4 including a noise reduction suite of landing gear and leading edge Krueger slat technologies (Refs 1, 17).

Therefore, the purpose of this section is to first estimate the noise reduction possible, within the N+2 framework, for the B27 if configured with the lower noise GTF (BPR ~15) from the fuel burn assessment of Section VII. Second, to then make a preliminary comparison of how these two leading unconventional advanced aircraft concepts, the B27 and the BWB, could compare as measured by the N+2 fuel burn and noise metrics and based on the latest analysis in this study and in Ref 17.

For the B27, the change in engine from the direct drive BPR 13.5 engine to the geared BPR 15 engine represents a significant change to the engine source levels. The fan pressure ratio is a more significant parameter for the dominate fan noise component of these engines and drops from 1.6 for the direct drive to 1.375 for the geared engine. The engine source noise can be lowered by as much as 10 EPNLdB cumulative for this magnitude of a drop in fan pressure ratio as can be seen in Ref 36, albeit for a smaller class of aircraft and a different mission.

In addition, optimizing the engine location relative to the position over the trailing edge of the wing may further increase the benefit of noise shielding. The B27 configuration studied here has not been optimized for maximum shielding effectiveness. Instead, the engine location on the baseline B27 was determined by other requirements such as the aerodynamic-propulsion integration, aircraft weight balance and stability control, and engine operability. Even small changes in the relative position can be significant on propagation to angles directly under the aircraft.

As a result of these further changes, it can be estimated that the B27 with GTF engines could reach as low as 40-42 EPNLdB below Stage 4 and left as a range until further analysis can be completed.

One specific technology that is included in the suite for the B27 but was not included in the suite for the BWB is the Over-the-Rotor and Soft Vane acoustic liner treatment. For comparison purposes, an estimate is made for the addition of the same treatment on the BWB aircraft of Ref 1.

Table 14 summarizes these preliminary estimates for the potential of these two different unconventional configurations with advanced technologies. While this estimate of the potential for low noise is very promising for the B27 with GTF engines it must be emphasized that further analysis is necessary and is in planning in order to rigorously assess this final technology configuration. Likewise, while the comparison between the noise of the BWB and the B27 is indicative of how close both can be, again, further analysis is planned to insure equivalent assumptions particularly for the noise reduction suite of technologies. Also note, the engine technologies are still not equivalent between the two concepts with a difference in BPR and fan pressure ratio.

Table 14. Preliminary Estimate of System Level Metrics for Similar B27 and BWB Aircraft

Metric	0009A NG AAT BWB of Ref. 1 with OTR/SV treatment added (GTF BPR 18, FPR 1.25)	B27 with GTF and noise reduction suite, current study (GTF BPR 15, FPR 1.375)
Noise, dB cumulative relative to Stage 4, *estimated	43-45*	40-42*
Fuel burn reduction relative to Boeing 1998 baseline aircraft model	53.7%	47.5%

IX. Conclusions

A detailed assessment has been presented on the system noise and fuel burn potential of an advanced tube-and-wing aircraft design with turbofan engine propulsion. The design innovates on the conventional tube-and-wing configuration with the engines mounted from a double deck fuselage at the mid-fuselage position behind and above the wings to take advantage of engine inlet fan noise shielding.

It has been shown that the baseline aircraft concept studied here can achieve a cumulative EPNL level about 28 dB below the current noise regulations of Stage 4, which makes the configuration acoustically viable in meeting current and anticipated noise regulations, as well as competing with other aircraft designs. The low noise levels result from a combination of various features and technologies incorporated on the baseline design. These included the direct-drive engine with a bypass ratio of 13.5 greatly reducing the jet noise, advanced duct liner technologies suppressing the fan tonal noise, the efficient wing design lowering the aircraft approach speed and the overall airframe noise, Krueger slats (sealed on takeoff, open on approach) eliminating slat cove flow separation, and the continuous flaps minimizing flap side edge noise. In addition, the unique engine/airframe integration leads to the absence of wing reflection of engine exhaust noise and the shielding of engine inlet noise by the wings, and fuselage shielding of engine noise in the sideline direction. It has been shown that this mid-fuselage mount configuration provides more than 4 EPNLdB advantage over an equivalent engine-under-the-wing configuration.

Within the NASA N+2 framework, goals, and consistent with similar recent studies, the potential of the B27 configuration was developed with two additional approaches. First, a suite of noise reduction technologies was added to the baseline design that when applied together reduced the noise to a level of 36 EPNLdB below Stage 4. This additional suite of technologies included Over the Rotor and Soft Vane liner treatment, scarf exhaust nozzle, sealed slat gap on both takeoff and approach, chevron nozzle, landing gear fairings, additional high lift wing

optimization, and porous flap side edge. And for the second approach, a preliminary estimate of the B27 with a higher bypass ratio GTF engine indicated that the concept could reach as low as 40-42 dB pending further analysis in progress.

A fuel burn assessment of the compete configuration with the GTF engines and including the noise reduction suite of technologies yielded a fuel burn reduction of between 43-47% relative to 2005 best-in-class aircraft, depending on the baseline used.

Further analysis is planned within the next year that will refine the B27 specifications to the N+2 technology suite and to better match the GTF with the B27 at improved scale factors. The new analysis is expected to provide a more precise measure of the potential of the B27 against the N+2 fuel burn and noise reduction goals. In addition, this will allow an improved and more consistent comparison with other advanced aircraft concepts such as the BWB.

At this stage, this fuel burn and noise assessment study clearly shows that the B27 concept is a promising advanced aircraft concept that is very competitive when measured by the NASA N+2 metrics. As with other similar studies this conclusion assumes that the many technologies included in the aircraft concept are all matured to full success within the timeframe and can be successfully integrated in a future embodiment of this aircraft concept. This point emphasizes the continued need for a vigorous research and development effort in order for the N+2 goals to be realized in future aircraft serving the public.

Acknowledgments

The authors thank the NASA Environmentally Responsible Aviation Project, Dr. Fay Collier, Project Manager, for funding this research.

References

1. Bonet J. T., Schellenger H. G., Rawdon B. K., Elmer K. R., Wakayama S. R., Brown D. & Guo Y. P. "Environmentally Responsible Aviation (ERA) Project – N+2 Advanced Vehicle Concepts Study and Conceptual Design of Subscale Test Vehicle (STV)," NASA Contract Report 2013-216519, 2013.
2. Bonet, J.T., "Boeing ERA N+2 Advanced Vehicle Concept Results," presentation at the 50th AIAA Aerospace Sciences Meeting, January 11, 2012, Nashville, Tennessee.
3. Guo Y. P. & Thomas R. H. "System Noise Assessment of Blended-Wing-Body Aircraft with Open Rotor Propulsion," SciTech Conference (National Harbor, Maryland), American Institute of Aeronautics and Astronautics, Reston, VA, 2014, (submitted for publication).
4. Collier, F.S., "Environmentally Responsible Aviation (ERA) Project," presentation at the Third NASA Fundamental Aeronautics Program Annual Meeting, September 29-October 1, 2009, Atlanta, Georgia.
5. Hill, G.A., and Thomas, R.H., "Challenges and Opportunities for Noise Reduction Through Advanced Aircraft Propulsion Airframe Integration and Configurations," presented at the 8th CEAS Workshop on Aeroacoustics of New Aircraft and Engine Configurations, Budapest, Hungary, Nov. 11-12, 2004.
6. Czech, M. J., Thomas, R. H., and Elkoby R., "Propulsion Airframe Aeroacoustic Integration Effects of a Hybrid Wing Body Aircraft Configuration," *International Journal of Aeroacoustics*, Vol. 11 (3+4), pp. 335-368, 2012.
7. Thomas, R. H., Burley, C. L., and Olson, E. D., "Hybrid Wing Body Aircraft System Noise Assessment with Propulsion Airframe Aeroacoustic Experiments," *International Journal of Aeroacoustics*, Vol. 11 (3+4), pp. 369-410, 2012.
8. Imamura, T., Ura, H., Yokokawa, Y., Enomoto, S., Yamamoto, K., and Hirai, T., "Designing of Slat Cove Filler as a Noise Reduction Devices for Leading-Edge Slat," AIAA 2007-3473.
9. Guo, Y. P., "A Discrete Vortex Model for Slat Noise Prediction" AIAA Paper 2001-2157, 2001.
10. Guo, Y. P., Pitera, D. M., Pitt, D. M., Shmilovich, A., and White, E. V., "Multi-Objective Leading Edge Concepts," Contract: NAS1-NNL04AA11B, TASK NNL08AD73T, June 29, 2009.
11. Guo, Y. P., "On Noise Reduction by Flap Side Edge Fences," *Journal of Sound and Vibration* **277**, 369-390, 2004.
12. Storms, B.L., Takahashi, T.T., Horne, W.C., Ross, J.C., Dougherty, R.P., Underbrink, J.P., "Flap-tip treatments for the reduction of lift-generated noise," NASA CDTM-21006, 1996.
13. Hutcheson, F. V., Brooks, T. F., and Humphreys, W. M., "Noise Radiation from a Continuous Mold-Line Link Flap Configuration," AIAA 2008-2966, 2008.
14. Ravetta, P. A., Burdisso, R. A., Ng, W. F., Khorrami, M. R., and Stoker, R. W., "Screening of Potential Noise Control Devices at Virginia Tech for QTD II Flight Test," AIAA 2007-3455, 2007.

15. Dobrzynski W., Chow L. C., Smith M., Boillot A., Dereure O., and Molin N., "Experimental Assessment of Low Noise Landing Gear Component Design," AIAA Paper 2009-3276, 2009.
16. Dobrzynski W., Chow L. C., Guion P., and Shiells, D., "Research into Landing Gear Airframe Noise Reduction," AIAA 2002-2409, 2002.
17. Guo, Y.P., Burley, C.L., and Thomas, R.H., "On Noise Assessment for Blended Wind Body Aircraft," SciTech Conference (National Harbor, Maryland), American Institute of Aeronautics and Astronautics, Reston, VA, 2014, (submitted for publication).
18. Guo Y. P. "A statistical model for landing gear noise prediction," *Journal of Sound and Vibration* **282**, 61-87, 2004.
19. Guo Y. P., "A component-based model for aircraft landing gear noise prediction," *Journal of Sound Vibration* **312**, 801-820, 2008.
20. Guo Y. P., "On Trailing Edge Noise Modeling and Prediction for Aircraft High Lift Wings," NASA Contract Report NASA Contract NNL07AA03A, 2010.
21. Guo Y. P., "Aircraft Slat Noise Modeling and Prediction," AIAA Paper 2010-3837, 2010.
22. Guo Y. P., "Slat Noise Modeling and Prediction," *Journal of Sound* Vibration. **331**, 3567-3586, 2012.
23. Guo Y. P., "Aircraft Flap Side Edge Noise Modeling and Prediction," AIAA Paper 2011-2731, 2011.
24. Guo Y. P., "Flap Side Edge Noise Modeling and Prediction," *Journal of Sound and Vibration*, **332**, 3846-3868, 2013.
25. Czech, M.,J., and Thomas, R.H., "Open Rotor Aeroacoustic Installation Effects for Conventional and Unconventional Airframes," AIAA Paper No. 2013-2185, presented at the 19th AIAA/CEAS Aeroacoustics Conference (Berlin, Germany), 2013.
26. Thomas, R.H., Czech, M.J., and Doty, M.J., "High Bypass Ratio Jet Noise Reduction and Installation Effects Including Shielding Effectiveness," AIAA Paper No. 2013-541, 2013.
27. Guo, Y.P., and Thomas, R.H., "System Noise Assessment of Blended-Wing-Body Aircraft with Open Rotor Propulsion," SciTech Conference (National Harbor, Maryland), American Institute of Aeronautics and Astronautics, Reston, VA, 2014, (submitted for publication).
28. Guo, Y. P., Czech, M. J., and Thomas R. H., "Open Rotor Noise Shielding by Blended-Wing-Body Aircraft," SciTech Conference (National Harbor, Maryland), American Institute of Aeronautics and Astronautics, Reston, VA, 2014, (submitted for publication).
29. Dowling, A. P. and Ffowcs Williams, J. E. 1983 *Sound and Sources of Sound.* Ellis Horwood Publishers.
30. Crighton, D.G., Dowling, A.P., Ffowcs Williams, J.E., Hekle, M., and Leppington, F.G., *Modern Methods in Analytical Acoustics.* Springer-Verlag, 1992.
31. Sutliff, D.L., Jones, M.G., Hartley, T.C., "Attenuation of FJ44 Turbofan Engine Noise with a Foam-Metal Liner Installed Over-the-Rotor," 15th AIAA/CEAS Aeroacoustics Conference, AIAA-2009-3141, 2009.
32. Jones, M., Parrott, T., Sutliff, D., Hughes, C., "Assessment of Soft Vane and Metal Foam Engine Noise Reduction Concepts," 15th AIAA/CEAS Aeroacoustics Conference, AIAA-2009-3142, 2009.
33. Mengle, V., Elkoby, R., Brusniak, L., Thomas, R., "Reducing Propulsion Airframe Aeroacoustic Interactions with Uniquely Tailored Chevrons, Part 2. Installed Nozzles," 12th AIAA/CEAS Aeroacoustics Conference (27th AIAA Aeroacoustics Conference), AIAA Paper No. 2006-2434, 2006.
34. Nesbitt, E., Mengle, V., Czech, M., Callender, B., Thomas, R., "Flight Test Results for Uniquely Tailored Propulsion-Airframe Aeroacoustic Chevrons: Community Noise," 12th AIAA/CEAS Aeroacoustics Conference (27th AIAA Aeroacoustics Conference), AIAA Paper No. 2006-2438, 2006.
35. McCullers, L., "Aircraft Configuration Optimization Including Optimized Flight Profiles," Proceedings of the Symposium on Recent Experiences in Multdisciplinary Analysis and Optimization, NASA CP 2327, April, 1984.
36. Guynn, M.D., Berton, J.J., Fisher, K.L., Haller, W.J., Tong, M.T., and Thurman, D.R., "Refined Exploration of Turbofan Design Options for an Advanced Single-Aisle Transport," NASA/TM-2011-216883, 2011.